Research Article

Songita Sonowal and Ram Prasad*

Exploring the effect of tea dust magnetic biochar on agricultural crops grown in polycyclic aromatic hydrocarbon contaminated soil

https://doi.org/10.1515/gps-2024-0109
received May 17, 2024; accepted October 17, 2024

Abstract: Magnetic biochar is a newly discovered novel material synthesized by adding an external magnetic field to conventional biochar. It exhibits dynamic properties like large surface area, porous cavities, ductility, and many functional groups on the surface. Due to the presence of these features, magnetic biochar has tremendous applications in various fields. The magnetic separation property is particularly beneficial for removing contaminants from soil. Much research has been done in this field, and positive results have been shown in the remediation of heavy metals, polycyclic aromatic hydrocarbons (PAHs), and organic contaminants from soil. Removal of these environmental contaminants is essential because they degrade the soil quality by alternating the physico-chemical activity and microbial diversity. Later, it makes the soil unfavorable for the growth of crops. Although much research has been done in this field and succeeded, little attention has been paid to the effect of magnetic biochar on plant growth. Therefore, in this research, we have synthesized the magnetic biochar from tea dust and applied it to the PAH-contaminated soil to explore the effect of tea dust magnetic biochar on the growth of barley plants.

Keywords: magnetic biochar, polycyclic aromatic hydrocarbons, barley

1 Introduction

Polycyclic aromatic hydrocarbons (PAHs) are noxious and oncogenic compounds that arise from the incomplete burning of fossil fuels and other natural resources [1]. When PAHs are exposed to the environment, soil quality is degraded by alternating the physico-chemical bonding of soil and destroying the microbial diversity. Later, through the root, it enters the plant body and causes some physiological changes that negatively impact the plant [2]. Usually, PAHs are predominantly found in the soil of crude oil drilling, coal mining, and other inorganic metal mining sites [3]. Therefore, in those regions, agricultural practices are not possible due to harsh and destroyed quality of the soil. The soil is degraded due to the loss of water-holding capacity and humus. From previous studies, it was found that the plants from the Poaceae family can grow in PAH-contaminated soil and remediate the PAHs from the soil, but accumulation of PAHs by the plants lowers the biomass, damages DNA, and alters the antioxidant system [4]. According to previous studies, plants grown in PAH-contaminated soil decrease the germination rate by causing damage to the cell membrane of the seeds. The majority of plants grown in PAH-contaminated soil are wild grass species (*Festuca rubra, Lolium perenne, Festuca arundinacea, Cynodon dactylon, Cyperus rotundus*, etc.) [4,5]. Once the plant absorbs PAHs, it interrupts the photosynthesis system by changing the structure of thylakoids, which leads to a disturbance in the electron transport system. Thus, the plants produce less chlorophyll content and suffer from malnutrition, which negatively affects the growth of plants. Moreover, when some low molecular weight PAHs enter the plant body, they lower the conductance of stomata and the maximum quantum yield in photosystem II [6]. Ultimately, contamination of PAHs not only inhibits the growth of plants but also reduces the yielding capacity of crops, which negatively impacts the food security and sustainable development of the

*** Corresponding author: Ram Prasad**, Department of Botany, Mahatma Gandhi Central University, Motihari, 845401, Bihar, India, e-mail: rpjnu2001@gmail.com
Songita Sonowal: Department of Botany, Mahatma Gandhi Central University, Motihari, 845401, Bihar, India

environment. Accumulation of high-dosage PAHs by the plants reduces the length of root and shoot, and due to this the biomass of plants also decreases [7]. Accumulation of PAHs by plants not only inhibits the plant growth but also affects the secondary metabolism, especially in those plants which produce flavonoids and phenolic acids [8].

The addition of magnetic biochar to the PAH-polluted soil can reduce the toxicity of PAHs in plants. A newly discovered engineered biochar was synthesized by adding magnetic precursors into the conventional biochar [9]. Magnetic biochar has a large surface area, porous cavity, and many functional groups on the surface [10]. Therefore, it has various applications in different fields, especially in environmental remediation [11–13]. When magnetic biochar is applied in the agricultural field, it improves the quality of soil by enhancing the microbial diversity and nutrients. In some recent studies, it has been reported that the use of magnetic biochar in agricultural soil increases the uptake of nitrogen and phosphorus by plants [14]. Moreover, it induces seed germination by releasing phytotoxins and karrikins and increasing the water holding capacity in the soil. Karrikin-associated biochar helps to overcome the dormancy period in some hard-coated seeds by changing the physiology and composition of plants [15]. As magnetic biochar has different types of elemental compositions on the surface, the application of magnetic biochar increases the growth of plant seedlings. The ion exchange capacity of magnetic biochar can improve the physico-chemical properties of soil and reduce the PAH toxicity by absorption. Previous studies revealed that magnetic biochar helps plants to mitigate abiotic stress like drought, salinity, and heavy metal and organic contaminant toxicity [16]. Dai et al. reported that biochar increases the heavy metal translocation in *Hordeum vulgare* L. [17]. Also, it was found that when it is applied in ornamental plants as a fertilizer, it increases the chlorophyll content, biomass, leaf area index, and blossom frequency of the plants [18].

Until now, many studies have been carried out on bioremediation assisted by conventional biochar and its effect on the growth of plants. However, little attention has been paid to its impact on the growth of agricultural crops under the stress of PAH-contaminated soil. Although PAH-contaminated soil has various side effects on plants and human health, this topic is still undervalued by researchers. Therefore, this research was carried out to synthesize magnetic biochar from tea dust waste and to investigate the effect of newly synthesized tea dust magnetic biochar (TMBC) on the growth of barley (*Hordeum vulgare*) plants in PAH-polluted soil.

2 Materials and methods

2.1 Chemical products used in the experiment

Ferric chloride ($FeCl_3$) and ferrous chloride ($FeCl_2$) were obtained from SRL (Sisco Research Laboratories Pvt. Ltd.); PAHs (napthalene and phenanthrene) were obtained from the Merck Co.; analytical grade acetone, ethanol, and sodium hydroxide solutions were obtained online from Ibuychemikals.

2.2 Synthesis of magnetic biochar

To synthesize magnetic biochar, tea dust was gathered from different tea factories in Assam, washed with tap water to remove dirt, and air dried overnight. Following cleaning, it was pyrolyzed for 60 min at 300°C in a muffle furnace. Afterward, the coprecipitation process was used to transform biochar into magnetic biochar (Figure 1). A 250 mL Erlenmeyer flask was usually filled with 100 mL of deionized water, 5.40 g of ferrous chloride, and 4.0 g of ferric chloride. The solution was then magnetically shaken continuously for 30 min. About 10 g of biochar was added to the mixture after 30 min, and it was agitated for further 30 min. After an hour of shaking, the pH was adjusted to 10–11 by adding the necessary amount of NaOH solution, and the mixture was once more shaken for an hour in a magnetic stirrer. Later, ethanol and deionized water were used to wash the magnetic biochar after it had been filtered and collected. Filtered TMBC was later stored in a polypropylene bag after being dried overnight at 70°C in a vacuum oven [19].

2.3 Characterization of magnetic biochar

An external magnetic field was used to determine the magnetic nature of the synthesized particles. The synthesized TMBC was characterized at the Central Instrumentation Facility in India. Scanning electron microscopy (SEM) with energy-dispersive X-ray spectroscopy (EDS), Fourier transform infrared (FTIR) spectroscopy, Brunauer–Emmett–Teller (BET) analysis, X-ray diffraction (XRD), vibrating sample magnetometry (VSM), and X-ray photoelectron spectroscopy (XPS) were done to characterize the TMBC. The morphological view and elemental composition of TMBC were analyzed with the help of SEM coupled with EDS. A scanning electron

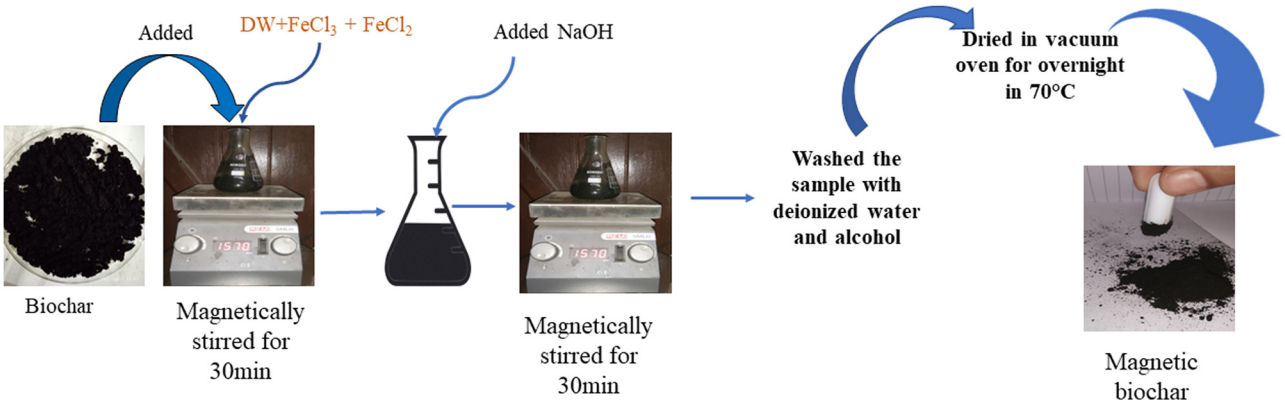

Figure 1: Diagrammatic representation of magnetic biochar synthesis.

microscope is an immensely powerful scientific instrument that uses a focused electron beam to produce three-dimensional, high-resolution images that review the surface topography of objects. With this method, one can gain unmatched insights into the minute features of nanoscale microstructures. The scanning electron microscope produces signals on solid specimens by using high-energy electrons, which disclose details about the materials crystalline structure, chemical makeup, and exterior appearance. Combining these details, a two-dimensional image is produced. In this technique, data are carefully gathered across a predetermined area, allowing researchers to investigate and comprehend the finer details of materials at a level never before possible [26]. Electron microscopy studies of TMBC were carried out by field-emission scanning electron microscopy (FESEM) (model: Sigma). For the study of the surface morphology and surface microstructures of the sample, a pinch of the sample was sputter-coated with gold in "times gold" mode with a sputter-current of 20 mA and a sputter-time of 59 s. FTIR was used for the identification and investigation of molecular amalgams based on their exclusive IR absorption spectra. Functional groups of the compounds were characterized with the help of FTIR; the surface area and pore size were measured by the BET method. The crystallinity of TMBC was observed with the help of XRD, and VSM and XPS were used to analyze the magnetization properties and surface elemental composition, respectively.

2.4 Experimental setup

The experiment was done closely following the procedure described by Zhen et al. with some minor changes [20]. Initially, the soil was obtained from the garden of Mahatma Gandhi Central University in Motihari, Bihar, India (26.6465°N, 84.9059°E). Motihari falls under the district of East Champaran and in the range of the northern hemisphere. In this area, the temperature is very high in June and recorded up to 46°C and very cool in January (6–13°C). The average annual rainfall of Motihari is about 1,200 mm [21]. The soil of Motihari is highly fertile and suitable for agricultural practice, has a pH of 7.5, an electrical conductivity of 1.12 dsm^{-1}, an organic carbon content of 0.35%, a nitrogen content of 165 $kg{\cdot}ha^{-1}$, a phosphorus content of 22.5 $kg{\cdot}ha^{-1}$, and a potassium content of 165 $kg{\cdot}ha^{-1}$. The collected soil was homogenized through a 2 mm screen and subjected to three rounds of autoclaving at 121°C. The experiment included three treatments, each with three replicates, amounting to nine plastic pots for plant cultivation, each containing 200 g soil [20].

In the first treatment (control), only soil and barley plants were included. The second treatment involved soil, plants, and PAHs (Soil + PAH), while the third treatment included soil, plants, PAHs, and synthesized TMBC (Soil + PAH + TMBC). To create the PAH solution, 0.15 g of PAHs (naphthalene and phenanthrene) was dissolved in acetone (300 mL), and 50 ppm from the stock solution was added to each pot during the second and third treatments for contamination, following the procedure described by Alves et al. [22].

After contaminating the soil, the third treatment pots were manually mixed with synthesized TMBC (5–10 wt%) as per Zhen et al.'s study. The pots were then placed under a laminar hood for 8 h to allow the organic solvents to evaporate. Barley seeds, pre-soaked overnight in test tubes, were sown into the treated soil with 25 seeds in each pot. Regular watering, administered using a spraying bottle, was performed as needed for optimal plant growth [20]. After 14 days of planting, barley plants were harvested at the growth stage, and physiological parameters and germination rates were assessed in PAH-contaminated soil.

2.5 Plant performance

The performance of barley plants was assessed based on morphological parameters. Root and shoot lengths of the barley plants were assessed during the 14-days growth stage, following harvest. Plant samples underwent a 72-h drying process at 70°C in a hot air oven to determine their dry weight. To calculate the relative water content, 0.2 g of barley leaves was incubated in 50 mL distilled water for 4 h from each treatment. The turgid weight of the leaves was measured after this incubation period. Subsequently, samples were subjected to a 48-h oven-drying process at 60°C [23]. Following the drying process, the weight was measured, and this value is incorporated into the formula to ascertain the relative water content of barley leaves [24]

$$\text{Relative water content (RWC) (\%)} = \frac{\text{Fresh weight} - \text{Dry weight}}{\text{Turgid weight} - \text{Dry weight}} \times 100$$

The chlorophyll content of the barley was also determined using Arnon's method (1949). 1 g of freshly cut barley leaves was ground using a clean mortar and pestle with 20 mL of 80% acetone. Then, the samples were centrifuged at 5,000 rpm for 5 min, and the supernatant was placed in a 100 mL volumetric flask. The same procedure was repeated until the residue became colorless. After that, the supernatant was collected in a flask and made up to 100 mL by adding 80% acetone. Then, the absorbance of the solution was read at 645 nm and 663 nm [25].

2.6 Statistical analysis

All statistical analyses were done using XLSTAT2014.5.03. ANOVA (analysis of variance) was done to analyze the difference between the treatments, and the least significant difference (LSD) test was done to compare the mean values at $P < 0.05$.

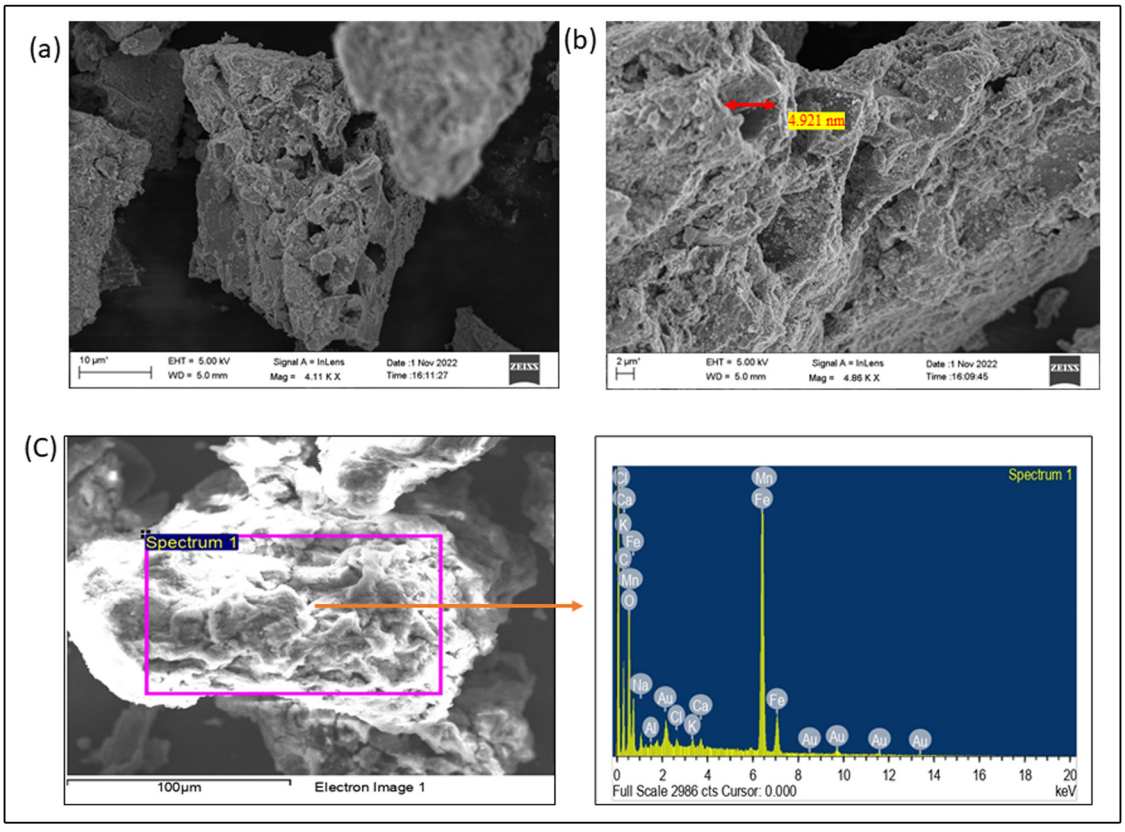

Figure 2: Micrographs of TMBC: (a) overview of TMBC under a scanning electron microscope, (b) higher resolution pore structure of TMBC, and (c) EDS analysis of TMBC.

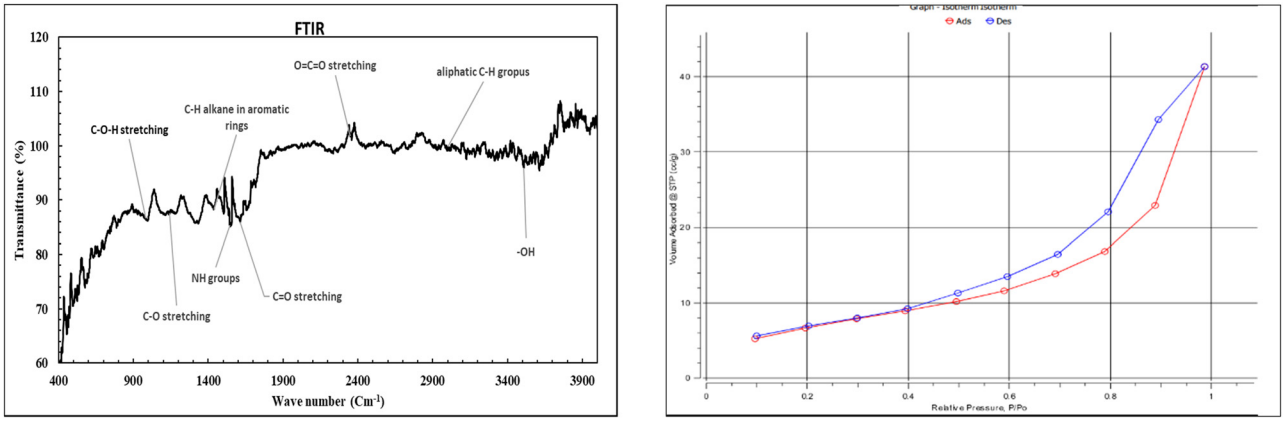

(a) (b)

Figure 3: (a) FTIR spectra of TMBC and (b) BET isotherm of TMBC.

3 Results and discussion

3.1 Characterization

SEM uses a focused electron beam to produce three-dimensional, high-resolution images that analyze the surface topography of objects [26]. As shown in Figure 2(a), the topographical image of TMBC is revealed through FESEM analysis. Figure 2(b) shows a closer examination of the visible openings on the TMBC surface. Additionally, the asymmetry in both the size and structure of the magnetic biochar becomes apparent. The dimensions and configurations of these pores are typically influenced by the pyrolysis temperature and duration, highlighting the correlation between processing parameters and the resulting characteristics. By observing the topography of TMBC, it can be said that its porous cavity would help to encapsulate the PAHs into their cavity, and a large surface area also helps to absorb many PAHs from the soil. This helps the soil to become nutrient-rich and suitable for agricultural purposes.

EDS plays an important part in the characterization of magnetic biochar, offering a precise method to analyze and determine the elemental composition of this material. By detecting and quantifying X-rays emitted from the sample during interactions with high-energy electrons, EDS detects the elemental composition present in the core of TMBC [27]. Figure 2(c) illustrates diverse elemental compositions with varying weights and atomic percentages within the

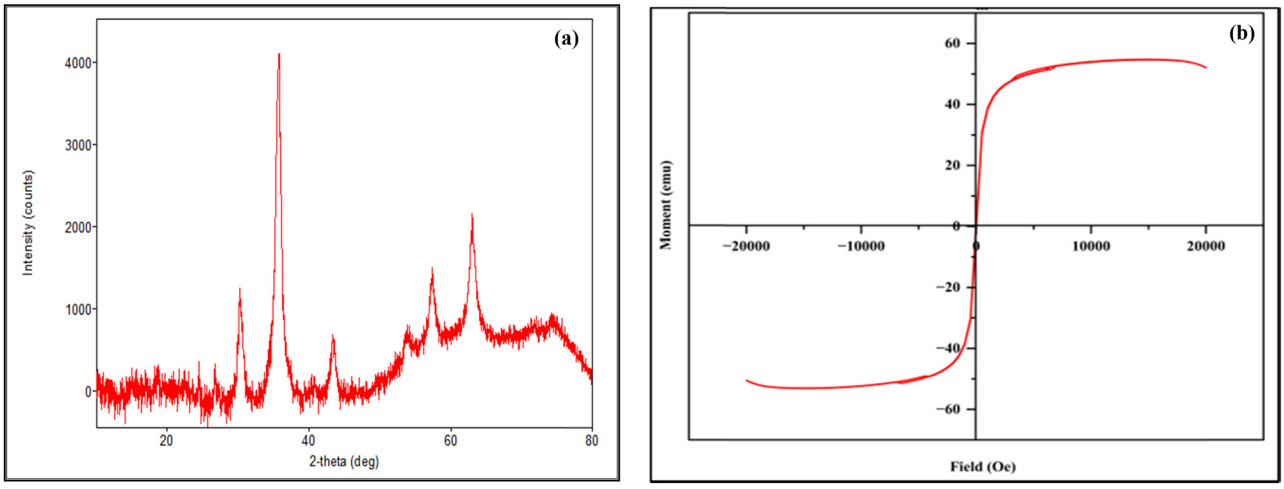

Figure 4: (a) XRD spectrum of TMBC and (b) magnetic saturation curve of TMBC.

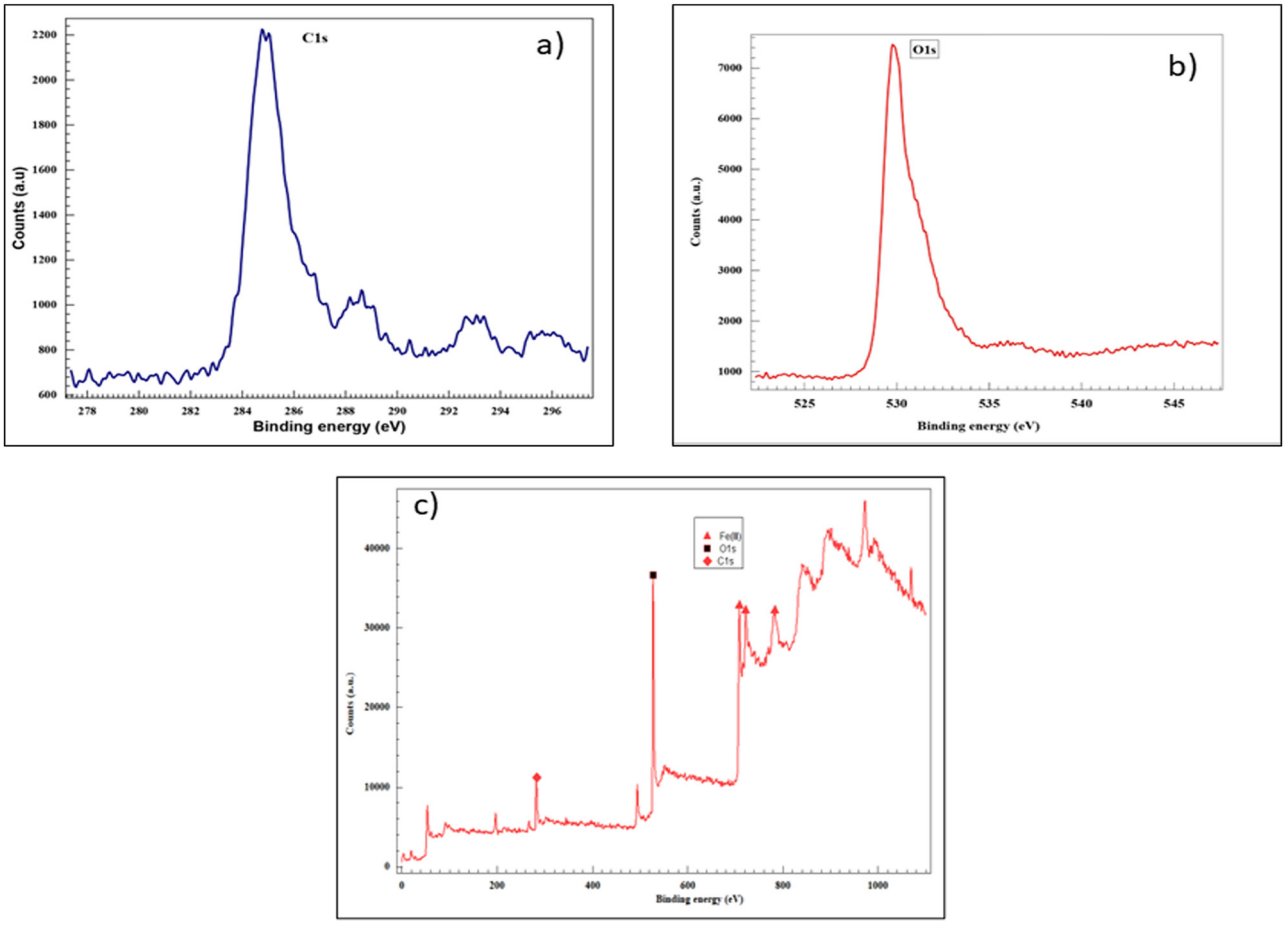

Figure 5: (a) High resolution C 1s XPS spectrum, (b) high resolution O 1s XPS spectrum, and (c) overall XPS spectrum of TMBC composition.

TMBC. The figure reveals that the TMBC consists of Fe, O, K, Mn, Cl, Ca, and C on the outer surface. Trace amounts of Na and Al are also identified through EDS analysis. Applying magnetic precursors $FeCl_2$ and $FeCl_3$ during biochar pretreatment leads to elevated levels of Cl and Fe. We can see that the concentration of Mn in the TMBC is very high; this may be due to that tea plants can absorb heavy metals in high amounts [28]. The biological feedstocks and pyrolysis temperature used to synthesize magnetic biochar vary the chemical composition of the magnetic biochar [29]. The elemental composition of TMBC positively influences the growth and development of plants. All the elements found in the TMBC are needed by the plants in either small or large amounts. For example, carbon is the main energy source of plants, iron is an important micronutrient in plants, which helps in the production of chlorophyll, and oxygen is important for cellular respiration, which promotes the seed germination of plants. Mn and Cl are also important micronutrients in plants that act as an activator and a co-factor of hundreds of metalloenzymes and chloroplast in plants. Likewise, K, Ca, and C also play an important role in the physiological activity of plants. K helps in the electrical neutralization of ions and anions. It also regulates the ion channels of the plasma membrane and cellular osmosis [30].

FTIR was used to analyze the functional groups present on the surface of TMBC. It is a simple, quick, and low-cost method for determining the occurrence of functional groups on the surface of magnetic biochar [31]. Figure 3(a) illustrates the FTIR spectrum of TMBC, covering a range from 3,900 to 400 cm^{-1}. The fingerprint region, delineated as the IR spectrum spanning from 1,200 to 700 cm^{-1}, is also featured [32]. A broad absorbance band, extending from 900 to 1,400 cm^{-1} is featured in the presence of C–O–H and C–O stretching in the spectrum [33]. The irregular peak detected in the series of 1,500 to 1,600 cm^{-1} is indicative of the –NH group, while the zigzag peaks at 3,500 cm^{-1} are distinctive features associated with the –OH group. The incorporation of C–H alkanes within aromatic rings leads to a spectrum overlap in the region spanning from 1,400 to 1,500 cm^{-1} [34]. The existence of an aliphatic C–H bond is suggested by a modest, rounded peak at 2,900 cm^{-1}.

A slight, piercing bent spectrum at 2,400 cm^{-1} indicates the potential occurrence of O═C═O stretching [35,36]. All the functional groups detected in TMBC is responsible for the immobilization of PAHs from the soil. Due to the ionic and anionic exchange capacity of functional groups present on the surface of magnetic biochar, the interaction between polyaromatic rings of PAH breaks. Gradually, the amount of PAHs is reduced in the soil due to the application of TMBC which makes the soil suitable for the growth of plants.

BET was used to analyze the surface area of solid or porous materials. BET measures the surface area of magnetic biochar depending on the nitrogen gas adsorption and desorption. The BET analysis of TMBC was measured in an St 1 on NOVAtouch 1LX [s/n: 17018081601] instrument at an ambient temperature 30.0926°C and a bath temperature 77.35 K. Figure 3(b) shows the nitrogen gas adsorption isotherm of TMBC, where the red isotherm represents adsorption and the blue isotherm represents desorption. The average pore size of TMBC is 4.9214e + 000 nm. The surface area of TMBC is 25.3902 $m^2 \cdot g^{-1}$. We can predict the adsorption capacity of PAHs in the soil from the pore size and surface. Because the surface area of TMBC is large, it means that it may have a large number of functional groups and elements on the surface.

The crystallinity and phase composition of TMBC were determined with the help of XRD. Figure 4(a) shows the XRD analysis of TMBC. A sharp and high peak was observed at the position of 2Θ (degree) of 35.682(15) from which it can be predicted that the sample is crystalline in nature. Many strong diffraction peaks were observed at 2Θ (degree) values of 53.71(9), 57.23(5), 63.03(4), 65.4(5), and 74.3(9) due to the presence of $FeCl_3$ and $FeCl_2$ in the TMBC. Due to the crystalline nature of TMBC, it will help in the photocatalytic degradation of PAHs in the soil. This is because the crystalline material has more photocatalytic activity than the amorphous material. It also positively influences the water holding capacity of soil which is beneficial for the plant growth [37]. The magnetization of TMBC was analyzed using a VSM instrument or Foner magnetometer. It measures the magnetic property of a sample based on the Faraday's law of induction. The sample was measured in a Lake Shore, model-7410 series VSM at MH_2T@300K. Figure 4(b) shows a saturation magnetization of TMBC of 54.63 $emu \cdot g^{-1}$ at room temperature, and from this we can predict that newly synthesized TMBC has the supermagnetic power which can remove the contaminants from the soil by magnetic separation.

XPS was done to analyze the chemical composition present on the surface of TMBC. Figure 5 shows the surface elemental composition of TMBC with their binding

Table 1: Mean values of some morphological parameters under three different treatments

Treatments	Shoot length (cm)	Root length (cm)	Fresh weight of plants (gm)	Dry weight of plants (gm)	% Seed germination	Relative water content (%)	Chlorophyll content of barley (645 nm)	Chlorophyll content of barley (663 nm)
Control	19.84 ± 0.88^{ab}	**19.70 ± 0.71	1.86 ± 0.032^{a}	0.34 ± 0.017^{a}	*66.67 (54.77 ± 2.90^{a})	**76.437 (61.028 ± 2.53^{a})	90.33 ± 4.09^{a}	85.40 ± 6.25^{a}
Soil + PAH	17.69 ± 0.39^{b}	**7.01 ± 0.52^{a}	*1.52 ± 0.079^{a}	0.20 ± 0.052^{a}	36.23 (36.90 ± 5.22^{b})	62.793 (52.431 ± 2.47^{b})	90.80 ± 7.69^{a}	90.71 ± 7.05^{a}
Soil + PAH + TMBC	*20.65 ± 0.17^{a}	8.32 ± 0.66^{a}	*3.66 ± 0.600	0.34 ± 0.045^{a}	*68.12 (55.69 ± 3.83^{a})	*71.787 (57.937 ± 1.75^{a})	99.57 ± 0.28^{a}	99.00 ± 0.50^{a}
Coefficient of variation	4.90	10.38	26.90	24.68	10.69	2.751	11.08	12.54
LSD (0.05)	2.15	2.75	1.43	N/A	11.914	3.563	N/A	N/A
LSD (0.1)	N/A	4.56	N/A	N/A	N/A	5.908	N/A	N/A

The data are shown as mean ± SE.
*Significant at 5%; **significant at 10%; N/A = not significant.
The mean values with different letters as superscripts is significant ($P < 0.05$). The mean values with the same letter or having a common letter(s) are not significantly different.
Figures in parentheses are angularly transformed values.

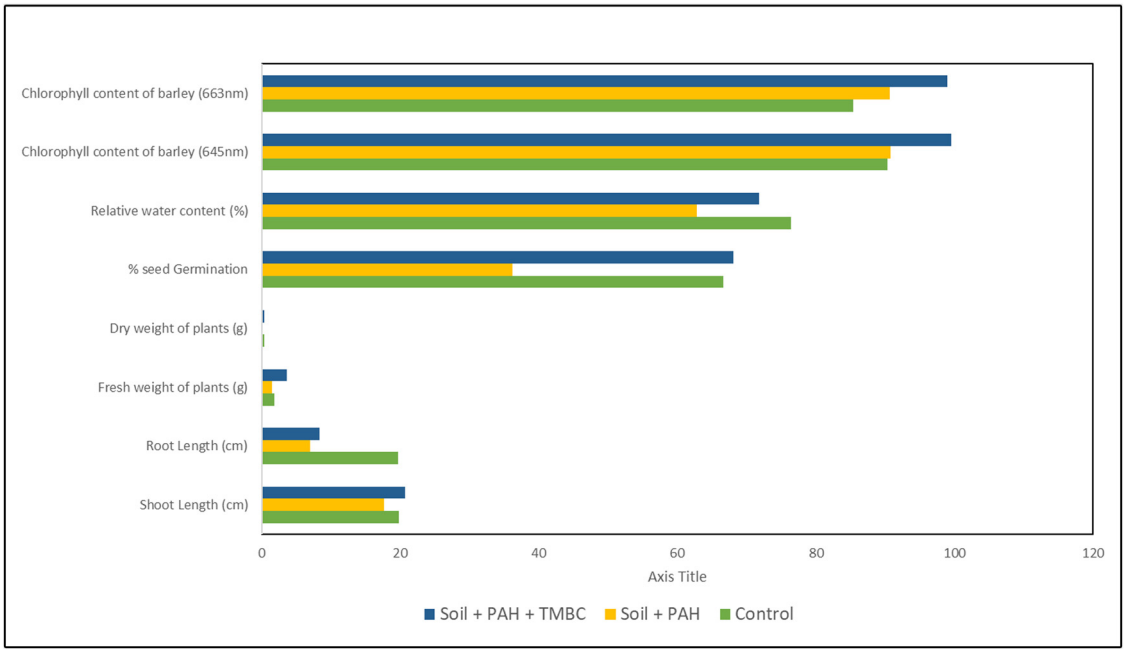

Figure 6: Effect of TMBC on the growth of barley plants.

energy. The figure reveals that the surface of TMBC has higher concentrations of C 1s and O 1s. Figure 5(a) and (b) shows the XPS high-resolution spectra of C 1s and O 1s, respectively. The C 1s XPS binding energy range is from 282 to 288 eV and the O 1s binding energy is between 530 and 535 eV. Figure 5(c) shows all the major surface elements of TMBC with their binding energy. Here, we can see that the concentration of O 1s is higher than that of C 1s in TMBC because the addition of magnetic precursors ($FeCl_3$ and $FeCl_2$) decreases the concentration of C 1s by increasing the concentration of O 1s. In this figure, the presence of Fe(III) is also detected in the range of 700–900 eV.

3.2 Plant performance

All the morphological characteristics are significantly affected by the combination of PAHs and TMBC in the soil. According to Table 1 and Figure 6, the control treatment shows the highest shoot, root length, and significant seed germination percentage (66.67%), which indicates the optimal conditions for barley growth without contamination. However, in the second treatment where PAH was added, the length of shoot and root and the weight biomass of barley were significantly reduced, which has a negative impact on the barley. However, the addition of TMBC in the PAH-treated soil shows an improvement in the root and shoot length and weight biomass. In terms of effect, the third treatment shows the highest mean shoot length (20.65 cm), which is higher than the 17.69 cm recorded in the second treatment. The relative water content and chlorophyll content of barley are also affected by the addition of PAHs and TMBC to the soil. The maximum relative water content is observed in the control group (76.43%), followed by the TMBC addition to soil. Notably, the chlorophyll content increased significantly in the Soil + PAH + TMBC treatment group compared to the control and Soil + PAH treatment groups; this indicates that adding TMBC enhances the photosynthetic efficiency under PAH stress. The coefficient of variation for different treatments indicated significant variability, especially in fresh weight (26.9) and dry weight (24.68%). The LSD values at a significance level of 0.05 showed notable differences between the treatments, especially between the control and Soil + PAH groups.

4 Conclusions

From the results, it is concluded that the existence of PAH in agricultural soil decreases the growth of crops. Toxic PAH contamination reduces soil fertility by destroying the physicochemical bonding of soil. Due to the hydrophobic nature of PAH, it repels soil water retention and disrupts the ecological balance, which negatively impacts

plant growth. However, the addition of newly synthesized TMBC into PAH-contaminated soil shows a positive effect on the growth of barley (*Hordeum vulgare*) and contributes to an enhancement in soil quality. Examining the topographies of the synthesized TMBC suggests that its porous structure plays a crucial role in capturing toxic PAHs, channeling them into its cavities, and transforming them into beneficial nutrients through the catalytic activity of functional groups. The magnetic nature of TMBC can easily separate the PAHs from the soil, and the functional groups present on the surface of TMBC help to catalyze the toxic PAHs by their ion exchange capacity. Moreover, the elemental composition detected in the TMBC enhances the plant's nutrient uptake by promoting plant root growth. In conclusion, it can be inferred that TMBC exhibits promising potential for fostering crop growth in soils contaminated with PAHs.

Acknowledgements: The authors express their gratitude to Mahatma Gandhi Central University, Motihari, Bihar, India, for providing the laboratory facilities to conduct this research. Ms. Songita Sonowal would like to thank the Ministry of Tribal Affairs for financial support. The authors want to express their heartfelt gratitude to Dr. Shwet Kamal (Principal scientist, ICAR – Directorate of Mushroom Research, Solan) for his invaluable assistance in statistical analysis of the data.

Funding information: The authors state no funding was involved.

Author contributions: Songita Sonowal drafted the manuscript, prepared the methodology, and carried out data collection and analysis. Ram Prasad edited the manuscript, conducted the investigation, and supervised the research work.

Conflict of interest: The authors state no conflict of interest.

Data availability statement: The datasets generated during and/or analysed during the current study are available from the corresponding author on reasonable request.

References

[1] Venkatraman G, Giribabu N, Mohan PS, Muttiah B, Govindarajan VK, Alagiri M, et al. Environmental impact and human health effects of polycyclic aromatic hydrocarbons and remedial strategies: A detailed review. Chemosphere. 2024;351:141227. doi: 10.1016/J.CHEMOSPHERE.2024.141227.

[2] Patel AB, Shaikh SK, Jain R, Desai C, Madamwar D. Polycyclic aromatic hydrocarbons: sources, toxicity, and remediation approaches. Front Microbiol. 2020;11:562813. doi: 10.3389/FMICB.2020.562813/BIBTEX.

[3] Wang H, Dong J, Long J, Jiang J, Lin C. Characteristics, sources analysis, and risk assessment of polycyclic aromatic hydrocarbon contamination in surface sediments surrounding tourist island. Mar Pollut Bull. 2024;206:116735. doi: 10.1016/J.MARPOLBUL.2024.116735.

[4] Sonowal S, Prasad MNV, Sarma H. C3 and C4 plants as potential phytoremediation and bioenergy crops for stabilization of crude oil and heavy metal co-contaminated soils-response of antioxidative enzymes. Trop Plant Res. 2018;5(3):306–14. doi: 10.22271/tpr.2018.v5.i3.039.

[5] Gawryluk A, Stępniowska A, Lipińska H. Effect of soil contamination with polycyclic aromatic hydrocarbons from drilling waste on germination and growth of lawn grasses. Ecotoxicol Environ Saf. 2022;236:113492. doi: 10.1016/J.ECOENV.2022.113492.

[6] Jajoo A, Mekala NR, Tomar RS, Grieco M, Tikkanen M, Aro EM. Inhibitory effects of polycyclic aromatic hydrocarbons (PAHs) on photosynthetic performance are not related to their aromaticity. J Photochem Photobiol. 2014;137:151–5. doi: 10.1016/J.JPHOTOBIOL.2014.03.011.

[7] Yang X, Hu Z, Liu Y, Xie X, Huang L, Zhang R, et al. Effect of pyrene-induced changes in root activity on growth of Chinese cabbage (Brassica campestris L.), and the health risks caused by pyrene in Chinese cabbage at different growth stages. Chem Biol Technol Agric. 2022;9(1):1–15. doi: 10.1186/S40538-021-00280-1/TABLES/2.

[8] Molina L, Segura A. Biochemical and metabolic plant responses toward polycyclic aromatic hydrocarbons and heavy metals present in atmospheric pollution. Plants. 2021;10(11):2305. doi: 10.3390/PLANTS10112305.

[9] Harikishore Kumar Reddy D, Lee SM. Magnetic biochar composite: Facile synthesis, characterization, and application for heavy metal removal. Colloids Surf, A. 2014;454(1):96–103. doi: 10.1016/j.colsurfa. 03.105.

[10] Tomin O, Yazdani MR. Production and characterization of porous magnetic biochar: before and after phosphate adsorption insights. J Porous Mater. 2022;1(1–11):849–59. doi: 10.1007/S10934-022-01217-1.

[11] Xiao B, Jia J, Wang W, Zhang B, Ming H, Ma S, et al. A review on magnetic biochar for the removal of heavy metals from contaminated soils: Preparation, application, and microbial response. JHM Adv. 2023;10:100254. doi: 10.1016/J.HAZADV.2023.100254.

[12] Sonowal S, Koch N, Sarma H, Prasad K, Prasad R. A review on magnetic nanobiochar with their use in environmental remediation and high-value applications. J Nanomater. 2023;2023(1):4881952. doi: 10.1155/2023/4881952.

[13] Rizwan M, Lin Q, Chen X, Li Y, Li G, Zhao X, et al. Synthesis, characterization and application of magnetic and acid modified biochars following alkaline pretreatment of rice and cotton straws. Sci Total Environ. 2020;714:136532. doi: 10.1016/J.SCITOTENV.2020.136532.

[14] Joseph S, Anawar HM, Storer P, Blackwell P, Chia C, Lin Y, et al. Effects of enriched biochars containing magnetic iron nanoparticles on mycorrhizal colonisation, plant growth, nutrient uptake and soil quality improvement. Pedosphere. 2015;25:749–60. doi: 10.1016/S1002-0160(15)30056-4.

[15] Kochanek J, Long RL, Lisle AT, Flematti GR. Karrikins identified in biochars indicate post-fire chemical cues can influence community

diversity and plant development. PLoS One. 2016;11(8):e0161234. doi: 10.1371/JOURNAL.PONE.0161234.
[16] Algethami JS, Irshad MK, Javed W, Alhamami MAM, Ibrahim M. Iron-modified biochar improves plant physiology, soil nutritional status and mitigates Pb and Cd-hazard in wheat (Triticum aestivum L.). Front Plant Sci. 2023;14:1221434. doi: 10.3389/FPLS.2023.1221434.
[17] Dai L, Chen Y, Liu L, Sun P, Liu J, Wang B, et al. Effect of biochar on the uptake, translocation and phytotoxicity of chromium in a soil-barley pot system. Sci Total Environ. 2022;826:153905. doi: 10.1016/J.SCITOTENV.2022.153905.
[18] Yan M, Tian H, Song S, Tan HTW, Lee JTE, Zhang J, et al. Effects of digestate-encapsulated biochar on plant growth. soil microbiome and nitrogen leaching. J Environ Manage. 2023;334:117481. doi: 10.1016/J.JENVMAN.2023.117481.
[19] Gao F, Xu Z, Dai Y. Removal of tetracycline from wastewater using magnetic biochar: A comparative study of performance based on the preparation method. Environ Technol Innov. 2021;24:101916. doi: 10.1016/J.ETI.2021.101916.
[20] Zhen M, Chen H, Liu Q, Song B, Wang Y, Tang J. Combination of rhamnolipid and biochar in assisting phytoremediation of petroleum hydrocarbon contaminated soil using Spartina anglica. J Environ Sci. 2019;85:107–18. doi: 10.1016/J.JES.2019.05.013.
[21] Geography of Motihari, Climate and Topography of Motihari. 2024. [Online]. https://motihari.biharonline.in/guide/geography-of-motihari.
[22] Alves WS, Manoel EA, Santos NS, Nunes RO, Domiciano GC, Soares MR. Phytoremediation of polycyclic aromatic hydrocarbons (PAH) by cv. Crioula: A Brazilian alfalfa cultivar. Int J Phytorem. 2018;20:747–55. doi: 10.1080/15226514.2018.1425663.
[23] Carter S, Shackley S, Sohi S, Suy TB, Haefele S. The impact of biochar application on soil properties and plant growth of pot grown lettuce (Lactuca sativa) and cabbage (Brassica chinensis). Agronomy. 2013;3:404–18. doi: 10.3390/AGRONOMY3020404.
[24] Farhangi-Abriz S, Torabian S. Effect of biochar on growth and ion contents of bean plant under saline condition. Environ Sci Pollut Res Int. 2018;25:11556–64. doi: 10.1007/S11356-018-1446-Z.
[25] Rajalakshmi K, Banu N. Extraction and estimation of chlorophyll from medicinal plants. IJSR. 2015;4(11):209–12.
[26] Burbano AA, Gascó G, Horst F, Lassalle V, Méndez A. Production, characteristics and use of magnetic biochar nanocomposites as sorbents. BMSBEO. 2023;172:106772. doi: 10.1016/J.BIOMBIOE.2023.106772.
[27] Scimeca M, Bischetti S, Lamsira HK, Bonfiglio R, Bonanno E. Energy dispersive X-ray (EDX) microanalysis: A powerful tool in biomedical research and diagnosis. Eur J Histochem. 2018;62:89–99. doi: 10.4081/EJH.2018.2841.
[28] Sarmah M, Borgohain A, Gogoi BB, Yeasin M, Paul RK, Malakar H, et al. Insights into the effects of tea pruning litter biochar on major micronutrients (Cu, Mn, and Zn) pathway from soil to tea plant: An environmental armour. J Hazard Mater. 2023;442:129970. doi: 10.1016/J.JHAZMAT.2022.129970.
[29] Wijitkosum S, Jiwnok P. Elemental composition of biochar obtained from agricultural waste for soil amendment and carbon sequestration. Appl Sci. 2019;9:3980. doi: 10.3390/APP9193980.
[30] Nieves-Cordones M, Al Shiblawi FR, Sentenac H. Roles and Transport of Sodium and Potassium in Plants. Met Ions Life Sci. 2016;16:291–324. doi: 10.1007/978-3-319-21756-7_9.
[31] Kong X, Liu Y, Pi J, Li W, Liao QJ, Shang J. Low-cost magnetic herbal biochar: characterization and application for antibiotic removal. ESPR. 2017;24:6679–87. doi: 10.1007/S11356-017-8376-Z/METRICS.
[32] Ramírez-Hernández A, Aguilar-Flores C, Aparicio-Saguilán A. Fingerprint analysis of FTIR spectra of polymers containing vinyl acetate. DYNA (Medellin). 2019;86:198–205. doi: 10.15446/dyna.v86n209.77513.
[33] Zhang N, Reguyal F, Praneeth S, Sarmah AK. A green approach of biochar-supported magnetic nanocomposites from white tea waste: Production, characterization and plausible synthesis mechanisms. Sci Total Environ. 2023;886:163923. doi: 10.1016/J.SCITOTENV.2023.163923.
[34] Pattanayek SK, Ghosh AK. Role of hydrogen bond interactions in water–polyol medium in the thickening behavior of cornstarch suspensions. Colloid Polym Sci. 2017;295:1117–29. doi: 10.1007/S00396-017-4107-8.
[35] Fan S, Li H, Wang Y, Wang Z, Tang J, Tang J, et al. Cadmium removal from aqueous solution by biochar obtained by co-pyrolysis of sewage sludge with tea waste. Res Chem Intermed. 2018;44:135–54. doi: 10.1007/S11164-017-3094-1.
[36] Shirvanimoghaddam K, Czech B, Tyszczuk-Rotko K, Kończak M, Fakhrhoseini SM, Yadav R, et al. Sustainable synthesis of rose flower-like magnetic biochar from tea waste for environmental applications. J Adv Res. 2021;34:13–27. doi: 10.1016/j.jare.2021.08.001.
[37] Asim N, Emdadi Z, Mohammad M, Yarmo MA, Sopian K. Agricultural solid wastes for green desiccant applications: an overview of research achievements, opportunities and perspectives. J Clean Prod. 2015;91:26–35. doi: 10.1016/J.JCLEPRO.2014.12.015.